Research Square

Preprints are preliminary reports that have not undergone peer review.
They should not be considered conclusive, used to inform clinical practice,
or referenced by the media as validated information.

Performance Limits of Low-Cost Extrusion for rPET Upcycling: A Study on Filament Quality, Strain-Rate Sensitivity, and Energy Absorption in 3D Printing

FR Wong
Universiti Teknologi MARA (UiTM) Shah Alam
MAA Ghani
mazimin@muscatuniversity.edu.om
Muscat University
Farrukh Jamil
Muscat University
Murid Hussain
Muscat University
Ala'a H. Al-Muhtaseb
Sultan Qaboos University
Ahmad Adli Zulkifli
Universiti Teknologi MARA (UiTM) Shah Alam

Research Article

Keywords: 3D Printing, PET, Extrusion, Additive Manufacturing, Circular Economy, Material Characterization

Posted Date: March 25th, 2026

DOI: https://doi.org/10.21203/rs.3.rs-9026986/v1

License: This work is licensed under a Creative Commons Attribution 4.0 International License.
Read Full License

Additional Declarations: No competing interests reported.

Abstract

The exponential growth in global plastic consumption has intensified the demand for effective waste management solutions, particularly for polyethylene terephthalate (PET) bottles. Converting post-consumer plastic waste into 3D printing feedstock offers a promising circular manufacturing pathway. However, adoption is constrained by the high cost of commercial filament extrusion systems. This study addresses this gap by presenting the design and fabrication of a low-cost filament extrusion system below RM 200, approximately USD 45, for recycling post-consumer PET (rPET) into 3D printing filament. Using off-the-shelf components, the system produced filament with diameters between 1.8 and 2.0 mm at an optimal extrusion temperature of 180°C. Mechanical testing showed that rPET achieved a tensile strength of 27 MPa compared to 35 MPa for PETG, with a Young's modulus of 0.215 GPa, indicating higher stiffness due to increased crystallinity. However, rPET exhibited reduced ductility below 9 percent and brittle failure at higher strain rates. These results indicate that rPET is suitable for static, non-structural applications. The novelty of this work lies in overcoming the cost barrier in rPET filament production through an affordable and easily replicable system that enables decentralized recycling and supports circular economy objectives under SDG 12.

1 Introduction

The high growth of plastic production and usage has resulted in a critical need for a solution to the present global environmental crisis. The total plastic waste produced worldwide every year exceeds 400 million tons of trash, of which a significant amount comprises packaging plastics, specifically PET bottles [1]. Despite being a lightweight, semi-transparent plastic material having high strength properties, the high level of single use of the material has resulted in significant landfilling of the material. A critical need for the design of a circular economy for the material has thus arisen.

Studies of policy analysis in the context of the European Union have shown that economic, technological, and ecological factors need to be integrated for the successful application of the large-scale material cycle to take place [2]. The processing of PET into a practical feed material to produce products through Additive Manufacturing (AM) of plastics can be a feasible route for the achievement of the above goal. Additive Manufacturing or 3D printing started from the world of prototyping to the end goal of producing functional components in the automotive, biomedics, or consumer products industry. Despite the breakthrough in the field of Additive Manufacturing of plastics, the ecological sustainability depends on the type of material being extruded.

A large and expanding body of research supports the potential outlined above. A framework for the application of a circular economy to 3D printed plastics was presented by Zhu et al.[1] to prove the equal processing capabilities of recycled PET plastics to their virgin counterparts when optimized. In the same context, Rashwan et al.[3] have been able to extrude r-PET plastics utilizing twin-screw compounded processes. Their tensile strength was reportedly equal to existing commercially marketed products. Other examples of feasibility have been mentioned regarding polylactic acid PLA plastics [4].

Despite the above improvements, several significant barriers to the adoption of RP filaments remain. Filament-making machines in the industry are costly; on the other hand, processing machines in industrial settings involve the steps of pelletization, filtration, and drying, making them unsuitable for small-scale institutions or community workshops [5]. Low-cost extruders have been developed for RP applications. These extruders usually lack necessary temperature control, have improper filament sizing, or lack automation capabilities to overcome the extrusion difficulties [6, 7].

Most of the technical literature specifically focuses on either large-scale applications or chemically altered PET (glycol-modified PET) instead of direct physical recycle processes for bottle-grade PET. Related studies, for example, relate more to studies about unmodified PET [8]. Also, most of the research studies strive to test the material mechanically without focusing on cost-effectiveness. Recent reviews show the same trend of existing knowledge gaps; for example, Dong et al. [9] summarized the research on the recycled material for additive manufacturing. Aniulis et al. [5] specifically reviewed the quality control of filament production. The researchers pointed out the lack of synchronization of either temperatures or pulling speed as the main factors affecting the quality of the filament.

These points indicate that a simple, thermally stable, and cost-effective extruder may well serve to close the existing gap between research in the lab and community-scale recycling. Even the advancement of green polymer research, including the processing of recyclable polymer links [10], may well supplement research in the lab, even if chemical research faces great challenges in its application to the industry. Even now, the upcycling of existing PET by small extruders seems to have the greatest application in meeting the challenges of sustainability.

With the above context in mind, the current research endeavours to conceptualize the development of a low-cost plastic filament extruder that can produce 3D printing filament from discarded PET bottles. The proposed extruder contains a 12V DC motor, a temperature control circuit known as the W1209 temperature controller, a nozzle of 1.8mm in size, and the total cost of the setup would remain under RM200. The current research highlights the technical issue in the extrusion process while simultaneously fulfilling the social requirement for a more efficient tool for the application of the circular economy.

2 Materials and Methods

2.1 Materials

Consumer waste PET bottles were sourced from local waste streams, rinsed with deionised water, and oven-dried at 60°C for three hours to remove residual moisture. The bottles were then manually converted into continuous feedstock strips by cutting them into widths of 8–10 mm using a handheld stripping tool as shown in Fig. 1. Comparable bottle-to-strip preparation approaches have been widely reported in recent rPET extrusion research, particularly within low-cost and distributed-recycling systems [11, 12]. These PET strips were subsequently used as the input material for filament extrusion.

For comparison, commercial PETG filament (1.75 mm, eSUN®, China) was selected as the benchmark material in the mechanical testing stage. PETG is frequently used as a reference in additive manufacturing studies on recycled thermoplastics due to its reliable melt flow behaviour and reproducible tensile properties [13]. All PET and PETG materials were stored in airtight containers with silica desiccant to limit moisture absorption, as PET is highly susceptible to hydrolytic degradation during melt processing [14].

2.2 Extruder Design and Fabrication

A low-cost PET filament extruder was designed and fabricated using easily available materials, following principles demonstrated in distributed recycling and waste-to-filament extrusion research. The system consists of a 12 V DC gear motor for feeding, an aluminium heating barrel, a 40 W cartridge heater embedded in a steel hot-end block, and a machined 1.8 mm brass nozzle. Temperature was regulated using a W1209 thermostat module, providing ± 3°C stability. Thermostat-based temperature control is acceptable in low-cost extruders and has been reported in several PET and waste-plastic filament-manufacturing systems [11, 12].

A complete CAD model of the extruder, created using SolidWorks, is shown in Fig. 2. The design ensured proper alignment between the feeding mechanism, heating block, and nozzle while maintaining structural rigidity. Such CAD-based validation is commonly used to evaluate geometric constraints and thermomechanical layouts before fabrication in recycled polymer extrusion systems [11].

The fabricated prototype is presented in Fig. 3, illustrating the assembled feeding motor, heating zone, control unit, and frame components. Similar compact extruders have been reported in literature for PET recycling, where the focus is on reducing cost, simplifying maintenance, and enabling small-scale filament production [11, 12, 15].

2.3 Operating Principle and Extrusion Parameters

PET strips were manually fed into the extruder hopper, where they were gripped by a motor-driven mechanism and pushed into a heated aluminum barrel. The optimal processing temperature was set between 175–185°C, consistent with the melt-processing window for recycled PET and with extrusion parameters reported in recent experimental studies [14, 16, 17]. Temperatures below 175°C result in incomplete melting, whereas temperatures above 190°C increase the risk of thermal degradation, as demonstrated through DSC and TGA analyses in rPET extrusion research [14, 17].

Once melted, the PET flowed through the 1.8 mm brass nozzle, forming a continuous filament strand. The filament was cooled under ambient laboratory conditions (25–27°C) and manually wound. Manual pulling allowed better control of filament diameter, a technique commonly used in extrusion lines without active diameter-feedback systems [12, 18].

A simplified process flow, beginning with PET bottle cleaning and proceeding through strip preparation, melting, extrusion, cooling, and winding, is represented in Fig. 4. Filament diameter was measured at 10

cm intervals along samples of approximately 3 m length. Maintaining a diameter within 1.8–2.0 mm was important for consistent downstream 3D printing and aligns with diameter tolerances reported in recycled filament studies [14, 16].

2.4 Filament Preparation, 3D Printing, and Specimen Fabrication

The extruded PET filament was first dried at 70°C for four hours to minimise moisture absorption, which is known to negatively affect melt flow behaviour and mechanical strength in recycled PET materials [14, 18]. Drying prior to printing is a standard requirement for PET-based polymers due to their strong susceptibility to hydrolytic degradation at elevated temperatures [14].

Tensile test specimens were fabricated using a Creality Ender-3 V2 fused filament fabrication (FFF) printer, following the ASTM D638 Type V geometry. This geometry is widely employed in studies of recycled polymer additive manufacturing because it enables the accurate evaluation of low-volume and recycled-material feedstocks [13, 19, 20]. The PET and PETG specimens printed for mechanical testing are shown in Fig. 5.

The printing parameters were selected based on experimental optimisation studies of recycled PET filament, where the influence of nozzle temperature, print speed, layer height, and bed adhesion on tensile performance was systematically analysed [19, 21]. In this study, the PET specimens were printed using a nozzle temperature of 245°C, whereas the PETG specimens were printed at 230°C. A bed temperature of 70°C, a layer height of 0.20 mm, and 100% infill density were applied for all prints to ensure consistent part consolidation. The print speed was maintained at 45 mm/s, which balances extrusion stability and surface quality, particularly when processing recycled thermoplastics with slightly variable melt-flow characteristics [19, 21].

All printed specimens were visually inspected to confirm dimensional accuracy and the absence of voids or delamination, following recommended practices for preparing ASTM-compliant tensile specimens from recycled filament [13]. Only samples with acceptable geometry and surface continuity were selected for subsequent mechanical testing.

2.5 Mechanical Testing

Mechanical testing was conducted using a Shimadzu Servopulser universal testing machine equipped with a 5kN load cell, as shown in Fig. 6. Tensile tests were performed in compliance with the ASTM D638 type V specifications. These types of specifications for tensile tests have been largely applied for the determination of the mechanical properties of FFF printed thermoplastics, including r-PET and PETG [13, 14, 18].

The samples were held in place by pneumatic grips to prevent slippage. A crosshead speed of 1mm/min was used. This was in agreement with the speeds of the tensile test of the studies of the last few years

on recycled PET material [13, 14, 18]. Force displacement curves were recorded by the digital acquisition system of the machine, and these curves were used to obtain engineering stress-strain curves. The ultimate tensile strength, Young's modulus of elasticity, and elongation at break of the material were determined from the stress-strain curves. These obtained values have been compared to those obtained in the latest research studies evaluating the mechanical properties of rPET and other recyclable plastics [11, 13–16, 18, 19, 21].

3 Results and Discussion

3.1 Filament Quality

The resulting recycled PET filament from the low-cost extruder was of acceptable dimensional stability in terms of diameters ranging between 1.80 & 2.00 mm. These values are sufficient for a feed in the process of fused filament fabrication. Variations in the diameters can be explained by the nature of the control of the extrusion process. Variations in the melt flow can also be a factor. According to Ror et al. [22], the flake size in the case of post-consistency PET flakes tends to produce diameter variability of the extruded filament. The authors also concluded that the process of pellets makes the flakes in the recycled material have improved feed properties. Additionally, the material also produces a decent filament exhibiting technical strength variability. The above conclusion also indicates the feasibility of producing decent, mechanically strong recycled PET. The commercial-grade PETG filament used in the experiment was of a uniform diameter. Its surface was also polished.

3.2 Tensile Specimen Appearance

Figure 7 presents the PET and PETG specimens after the tensile test performed at speeds of 1, 3, and 5mm/min. The test results for the PET material show brittle failure without significant necking, representing a lack of plastic deformation capacity. On the contrary, the test results for the PETG material indicate a ductile failure mode, as evidenced by visible necking and elongation before failure. The different failure modes of the two materials correspond to their stress vs. strain curves. While the stress vs. strain curve for the PET sample suggests a steeper slope in the elastic region despite the small strain at break values, the curve for the PETG sample shows a significant plastic deformation region.

3.3 Tensile behaviour and strain sate sensitivity

The engineering stress–strain curves for the rPET and commercial PETG material, plotted at a crosshead speed of 1, 3, or 5 mm/min, are shown in Fig. 8. These stress–strain curves have deformation behaviour that is clearly affected by the macromolecular structure of the material.

The strain-rate effect on PETG is further quantified using toughness (strain energy density), which integrates the full deformation response and is presented in Fig. 9. The rPET material showed a purely elastic response trending to a sudden failure point without any visible plastic yield. With the increase of

the strain rates from 1 to 5 mm/min, the material was shown to be viscoelastic since the overall stiffness and maximum force values increased, but the failure strain values decreased. These properties show the tendency of rPET to become more brittle at higher rates of deformation. This was also linked to the nature of the material extrusion processes of general thermoplastics, in which the higher rates of loading delay the molecular chain relaxation. This makes the chain molecules of the material less movable. A material revealing the characteristics of rPET would show higher stiffness but reduced flexibility when subjected to dynamic loading.

Conversely, the behaviour of PETG was clearly ductile, having a clear yield point followed by well-defined plastic deformation. After the onset of yielding, the stress- strains exhibited a smooth transition to failure in both cases, all having a clear strain to failure of about 9%. Unlike rPET, the material remained ductile even at higher strain rates. This improved ductility can be largely attributed to the glycol-modified amorphous structure of the material that resists crystallization and promotes the dissipation of energy via plastic deformation [23]. Past studies have validated experimentally that PETG retains its toughness characteristics in different strain rates [24, 25], thus supporting the trends validated in the current analysis.

of 1, 3, and 5 mm/min.

3.4 PET–PETG Mechanical Comparison

The comparative stress vs. strain graphs of the recycled PET and the PETG shown in Fig. 10 above clearly reveal the different trade-offs of both materials in terms of their strength. While the stress vs. strain curve of the recycled PET exhibits a sharper slope indicative of higher values of the modulus of elasticity due to the semi-crystalline nature of the material, the lack of a yield point in the curve suggests a brittle material.

In a different manner, the transition of the PETG sample between the elastic region and the plastic region is more gradual. Even if the initial elasticity of the material is higher in terms of the slope of the curve in the elastic region, the material continues to have a steady plastic elongation process that includes significant strain hardening. As shown in the shaded regions in Fig. 10, the total area under the curve of the PETG sample greatly exceeds the total area under the rPET curve. This helps to verify the findings of Ghasemkhani et al.[26] about the importance of maintaining the amorphous structure in order to have the capability of elongation.

In general, the above analysis indicates that RPET is a stiff but brittle material for static load applications, while the combination of medium stiffness values and high ductility exhibited by PETG makes the latter suitable for the required application.

3.5 Failure Modes

The tensile failure behaviour of recycled PET (rPET) and commercial PETG exhibits fundamentally different characteristics, reflecting the distinct molecular structures and thermal histories of the two

materials. These differences are consistent with the qualitative specimen appearance observed after testing, Fig. 7 and are further clarified through fracture morphology analysis.

Commercial PETG specimens failed in a ductile manner, characterized by pronounced plastic deformation prior to fracture. The material exhibited localized necking, stress whitening, and gradual crack development, indicating effective stress redistribution during tensile loading. This behaviour is attributed to the glycol-modified amorphous structure of PETG, which suppresses crystallization and promotes high segmental mobility. As a result, the polymer chains are able to undergo extensive slippage and strain hardening before fracture, allowing the material to maintain ductility even at elevated strain rates. Similar strain-rate-insensitive ductile failure behaviour in additively manufactured PETG has been reported by Ergene and Bolat [24], supporting the observations in the present study.

In contrast, recycled PET consistently exhibited brittle failure, characterized by abrupt fracture without measurable plastic deformation. The fracture occurred with no visible necking or stress whitening, indicating limited molecular mobility and rapid crack propagation once the elastic limit was exceeded. This behaviour is associated with the semi-crystalline nature of rPET, where crystalline domains formed during repeated thermal processing restrict chain relaxation and inhibit plastic flow.

Detailed examination of the fracture surface at the highest applied strain rate (5 mm/min) further confirms this behaviour. As shown in Fig. 11, the rPET specimen exhibits a sharp, granular fracture surface with a clearly defined crack boundary and minimal surface roughening. The absence of fibrillation or drawn polymer ligaments indicates that failure occurred through rapid crack initiation and propagation rather than stable plastic deformation. Such fracture morphology is characteristic of mechanically recycled PET and has been widely reported in the literature, where increased crystallinity and molecular weight degradation promote brittle rupture and low energy absorption prior to failure [22].

Overall, the observed failure modes corroborate the tensile and toughness results discussed in the preceding sections. Recycled PET behaves as a stiff but brittle material with limited tolerance to dynamic or high-rate loading, whereas PETG retains ductility and energy dissipation capability across the tested strain rates. These contrasting failure mechanisms have direct implications for material selection in additive manufacturing applications, particularly where impact resistance or cyclic loading is a design consideration.

3.6 Toughness and Energy Absorption

The strain energy density, or modulus of toughness, was calculated from the stress–strain data using trapezoidal numerical integration in order to quantify the total mechanical energy absorbed prior to fracture. The results for all test conditions are presented in Fig. 12 and reveal a clear distinction in the rate-dependent energy absorption behaviour of recycled PET and PETG.

Recycled PET shows a decreasing trend in toughness with increasing strain rate. The toughness drops from 1.37 MJ/m³ at 1 mm/min to 0.91 MJ/m³ at 3 mm/min, and reaches the lowest value of 0.84 MJ/m³ at 5 mm/min. This reduction in absorbed energy indicates that recycled PET becomes increasingly brittle

as the deformation rate increases. The decline reflects the limited time available for molecular-chain relaxation during high-rate loading, which restricts plastic deformation and promotes premature crack initiation. This behaviour is consistent with the viscoelastic characteristics of semi-crystalline polymers, where higher strain rates suppress molecular mobility and shift the response toward brittle failure.

In contrast, PETG displays the opposite trend. Its toughness increases steadily with loading speed, rising from 1.47 MJ/m³ at 1 mm/min to 1.63 MJ/m³ at 3 mm/min, and reaching 1.75 MJ/m³ at 5 mm/min. At the highest strain rate, PETG absorbs approximately twice as much energy as recycled PET. This improved performance can be attributed to the capacity of PETG to maintain ductility and undergo strain hardening even under rapid loading. The predominantly amorphous, glycol-modified structure of PETG supports greater segmental mobility and delays the onset of brittle fracture. Similar improvements in energy absorption at higher deformation rates have been reported for amorphous thermoplastics processed through material-extrusion pathways, as noted by Petousis et al. [23].

Overall, the toughness results reinforce the contrasting mechanical behaviours observed in the previous sections. Recycled PET transitions toward brittle, low-energy failure at elevated strain rates, whereas PETG demonstrates enhanced energy absorption and sustained deformation capacity. These differences have important implications for the selection of materials in applications where components may be subjected to rapid or dynamic mechanical loading.

3.7 Modulus, Elongation, and Stiffness Comparison

A detailed analysis of Young's modulus of the material, elongation at break, and stiffness is given in Figs. 13 to 15. Figure 13 highlights the graphical representation of the obtained values of the Young's modulus taken from the initial parts of the stress vs. strain curves. The rPET material shown in the figure was stiffer compared to the PETG material. Its value varied between 0.19 GPa & 0.24 GPa in comparison to values ranging between 0.19 GPa & 0.21 GPa for the latter. An increase in the value of the stiff material has also validated the claim of Méndez et al. in their research work [27]. The study claimed that the tensile strength may decrease in the case of material regeneration, but the values of the modulus of the material may well increase.

Figure 14 represents the ductility ratio in terms of elongation at break. The values of elongation at break of the PETG sample have always been higher (8–9%) compared to rPET (6–9%). This result validates the Ergene & Bolat study about the improved ductility of PETG over rPET. Moreover, the improved ductility of PETG was due to the glycol-modified molecules in the main chain [24].

FInally, Fig. 15 show the approximate values of stiffness (force/displacement) for different speeds. The values indicate a sharp reduction in the stiffness of rPET material for higher strain rates. On the contrary, the material PETG exhibits comparable values of stiffness for all the speeds. The result of the decrement in the rPET material under dynamic load conditions proves the statement of Muñoz et al. [28] that the repeated cycles of thermal processing caused chain scission and a decrease in the molecular weights of

the PET material. This resulted in a material less competent to maintain the values of stiffness under different load rates.

3.8 Comparative Analysis and Structure–Property Relationships

The results of mechanical properties show that there is an intrinsic balance between stiffness and ductility caused by differences in molecular structure. In particular, the rPET filament had a greater Young's modulus of 0.215 GPa than that of commercial PETG of 0.200 GPa but showed much lower ductility. The rPET specimens were thus found to have an elongation of less than 9%.

The enhanced rigidity exhibited by the rPET material is primarily ascribed to the thermal history inherent to mechanical recycling. As established in studies by Méndez et al. [27] and Van de Voorde et al. [14], repetitive thermal processing triggers chain scission while simultaneously promoting the development of crystalline domains. Such crystalline regions serve to restrict segmental mobility, a mechanism that increases the modulus but inevitably inhibits plastic flow, thereby producing a brittle material response. Examination of the fracture morphology reveals rapid crack propagation and an absence of stress whitening, as shown in Fig. 12, characteristics that parallel the observations of Ror et al. [22]. Moreover, the abrupt rupture observed in the rPET samples is consistent with phenomena described by Nguyen et al. [29], where non-uniform melting of post-consumer flakes generates stress concentrators that precipitate premature failure.

On the other hand, the commercial grade of PETG demonstrated high ductility and toughness at every applied strain rate. This is because the material is glycol-modified, meaning that the comonomer affects the regularity of the chains and prevents the material from gaining the ability to undergo crystallization, thus remaining essentially in the amorphous state. Seno et al. [21], Ergene and Bolat [24] suggest that the inability of the material to undergo crystallization due to the amorphous nature helps in chain slippage and the consequent strain hardening, thus aiding in the effective energy dissipation during the material's plastic deformation. On the other hand, the rPET samples exhibited high strain rate sensitivity, where the toughness was lower as the loading rate was increased. The reduced toughness during dynamic loading is similar to the viscoelastic properties of rPET characterized by Petousis et al. [23] and the findings of the research undertaken by Muñoz et al. [28], where the decrease in the molecular weight, attained due to the recycling process, affects the material's capacity to reduce under dynamic loading conditions.

3.9 Implications for Additive Manufacturing

A well-defined application potential in the additive industry can be established by combining the performance differences of rPET and PETG materials with the effectiveness of the low-cost extrusion method.

The rPET filament's high stiffness and tensile strength make it ideal for non-structural applications where impact resistance isn't a primary design concern. It can be used for manufacturing jigs, conceptual

prototypes, and enclosures for electronics. This filament can be produced with a cost-effective extruder which helps substantiate the idea of distributed recycling. This supports Little et al. [11], stating that filament localization is crucial in minimizing the economic cost in adopting a circular economy. Additionally, Mishra et al. [30] pointed out that in situ recycling of functional 3D printing materials from waste PET divert significant e-transport load from global supply chains.

However, the snap-fit and dynamic load applications should be eliminated due to the limited toughness of rPET. In other engineering-grade components, due to high energy absorption, PETG will continue to be the better option. Nonetheless, rPET's environmental consideration is hard to argue against. Replacing virgin polymers, as Pires et al. [31] showed, with mechanically recycled PET in fused filament fabrication, fills an SDG 12 void and, when printing parameters are optimized to reduce brittleness, can lower the cumulative energy expenditure of printed components by as much as 40%.

Conclusion

This research shows that it is possible to move towards a closed-loop solution for post-consumer PET waste through the design and development of an inexpensive filament extruder (which costs under RM 200/USD 45). By localizing the design and minimizing thermal management requirements, it was possible to produce rPET filaments of diameters ranging from 1.8 mm to 2.0 mm. This was sufficient for FFF.

From mechanical property evaluation, it is noticeable that there exists a distinct difference between the recycled feedstock and commercial samples. A tensile strength of 27 MPa could be obtained from the 3D printed samples of rPET, which, while lower compared with 35 MPa for commercial PETG, is acceptable for non-structural uses. However, from assessment of property-structure relationships, it can be observed that while the value of Young's modulus for the rPET material is 0.215 GPa and the material displays less than 9% elongation and is highly sensitive to testing speeds, indicating a brittle response because of its crystalline nature and thermal properties, commercial PETG displays superior toughness and ductility at every testing speed, as indicated by its amorphous glycol modified structure.

In regard to sustainability issues, this research confirms that distributed recycling has been a feasible approach for achieving Sustainable Development Goal 12. However, with the absence of energy-absorption properties relevant to dynamic loading applications in recycled polyethylene terephthalate materials, this research suggests that stiffness and lower cost make rPET a suitable choice for purposes like conceptual design modelling and prototyping.

To further develop this system from a prototype to a fully functional production system, future research will focus on incorporating an automated spooling system, along with real-time diameter control feedback. This improvement is expected to help minimize the small variations in dimensional accuracy observed in the current experiment, thereby further enhancing the printability and mechanical properties of the recycled material.

Abbreviations

AM
Additive Manufacturing
ASTM
American Society for Testing and Materials
CAD
Computer–Aided Design
DC
Direct Current
DSC
Differential Scanning Calorimetry
FDM
Fused Deposition Modeling
FFF
Fused Filament Fabrication
GPa
Gigapascal
MJ/m^3
Megajoules per cubic meter
MPa
Megapascal
MEX
Material Extrusion
NTC
Negative Temperature Coefficient
PET
Polyethylene Terephthalate
PETG
Glycol–Modified Polyethylene Terephthalate
PLA
Polylactic Acid
rPET
Recycled Polyethylene Terephthalate
RP
Recycled Plastic
SDG
Sustainable Development Goal
TGA
Thermogravimetric Analysis

UiTM
Universiti Teknologi MARA

Declarations

Author Contribution

MAA Ghani: Conceptualization, literature review, data analysis, writing, and original draft. Farrukh Jamil: Data curation, supervision, writing, review & editing. FR Wong, Ahmad Adli Zulkifli: Writing, review & editing. Murid Hussain: Formatting, and writing. Ala'a H. Al-Muhtaseb: Resources, writing, and review & editing.

Acknowledgements

The author gratefully acknowledges the support provided by the School of Mechanical Engineering, College of Engineering, Universiti Teknologi MARA (UiTM), Malaysia, for facilitating the computational resources required to conduct this research. Appreciation is also extended to colleagues and reviewers whose constructive feedback has contributed to improving the clarity and quality of this work.

Data Availability

Data Availability StatementThe datasets generated and/or analyzed during the current study are available from the corresponding author on reasonable request.

References

1. Zhu C et al (Feb 27 2021) Realization of Circular Economy of 3D Printed Plastics: A Review. Polym (Basel) 13(5):744. 10.3390/polym13050744
2. Georgescu LP, Fortea C, Antohi VM, Balsalobre-Lorente D, Zlati ML, Barbuta–Misu N (2025) Economic, technological and environmental drivers of the circular economy in the European Union: a panel data analysis. Environ Sci Europe 37(1):1–30. 10.1186/s12302-025-01119-4
3. Rashwan O et al (Sep 25 2023) Extrusion and characterization of recycled polyethylene terephthalate (rPET) filaments compounded with chain extender and impact modifiers for material-extrusion additive manufacturing. Sci Rep 13(1):16041. 10.1038/s41598-023-41744-8
4. Aly R, Olalere O, Ryder A, Alyammahi M, Samad WA (Dec 20 2024) Mechanical Property Characterization of Virgin and Recycled PLA Blends in Single-Screw Filament Extrusion for 3D Printing. Polym (Basel) 16(24):3569. 10.3390/polym16243569
5. Aniulis J, Kryszak B, Grzymajło M, Dudzik G, Abramski KM, Szustakiewicz K (2024) Characterisation and manufacturing methods of material extrusion 3D printing composite filaments based on

polylactide and nanohydroxyapatite. Additive Manuf 94:104514. 10.1016/j.addma.2024.104514

6. Putra IR, Bukhori ML, Prasetiyo AB, Robbika F, Putra BT (2024) Recycled PET Plastics Filament: Characteristic and Cost Opportunity. Semesta Teknika 27(2):148–158. 10.18196/st.v27i2.21072
7. Omiyale B, Olugbade T, Farayibi PK, Kayode (2024) Waste Plastics to 3D Printer Filament: An Overview on Industrial Applications. J Eng Res 10:1587–1598
8. Iacob DV, Zisopol DG, Minescu M (Jun 13 2025) Study on the Optimization of FDM Parameters for the Manufacture of Three-Point Bending Specimens from PETG and Recycled PETG in the Context of the Transition to the Circular Economy. Polym (Basel) 17(12):1645. 10.3390/polym17121645
9. Dong Y, Li H, Wang L, Chen J, Sucala VI, Jiang J (2025) Review on Recycled Materials for Additive Manufacturing. Int J Precision Eng Manufacturing-Green Technol 1–32. 10.1007/s40684-025-00788-z
10. Highmoore JF, Kariyawasam LS, Trenor SR, Yang Y (2024) Design of depolymerizable polymers toward a circular economy. Green Chem 26(5):2384–2420. 10.1039/d3gc04215d
11. Little HA, Tanikella NG, M JR, Fiedler MJ, Snabes SL, Pearce JM (Sep 25 2020) Towards Distributed Recycling with Additive Manufacturing of PET Flake Feedstocks. Mater (Basel) 13(19):4273. 10.3390/ma13194273
12. Al Rashid A, Koç M (2024) Additive manufacturing for sustainability, circularity and zero-waste: 3DP products from waste plastic bottles. Compos Part C: Open Access 14:100463. 10.1016/j.jcomc.2024.100463
13. Mercado-Colmenero JM, La Rubia MD, Mata-García E, Rodriguez-Santiago M, Martin-Doñate C (2023) Using numerical-experimental analysis to evaluate rPET mechanical behavior under compressive stresses and MEX additive manufacturing for new sustainable designs. Rapid Prototyp J 29(11):98–116. 10.1108/rpj-10-2022-0371
14. Van de Voorde B et al (2022) Effect of extrusion and fused filament fabrication processing parameters of recycled poly(ethylene terephthalate) on the crystallinity and mechanical properties. Additive Manuf 50:102518. 10.1016/j.addma.2021.102518
15. Ragab A, Elazhary R, Schmauder S, Ramzy A (2023) Plastic Waste Valorization for Fused Deposition Modeling Feedstock: A Case Study on Recycled Polyethylene Terephthalate/High-Density Polyethylene Sustainability, *Sustainability*, vol. 15, no. 18, p. 13291. 10.3390/su151813291
16. Nikam M, Pawar P, Patil A, Patil A, Mokal K, Jadhav S (2024) Sustainable fabrication of 3D printing filament from recycled PET plastic, *Materials Today: Proceedings*, vol. 103, pp. 115–125. 10.1016/j.matpr.2023.08.205
17. Mi D, Zhang J, Zhou X, Zhang X, Jia S, Bai H (Dec 5 2023) Direct 3D Printing of Recycled PET/PP Granules by Shear Screw Extrusion. Polym (Basel) 15(24):4620. 10.3390/polym15244620
18. Atsani SI, Sing SL (Aug 16 2024) Optimization of Glass-Powder-Reinforced Recycled High-Density Polyethylene (rHDPE) Filament for Additive Manufacturing: Transforming Bottle Caps into Sound-Absorbing Material. Polym (Basel) 16(16):2324. 10.3390/polym16162324

19. O'Driscoll C, Owodunni O, Asghar U (2024) Optimization of 3D printer settings for recycled PET filament using analysis of variance (ANOVA), *Heliyon*, vol. 10, no. 5, p. e26777, Mar 15 10.1016/j.heliyon.2024.e26777
20. Bustos Seibert M, Mazzei Capote GA, Gruber M, Volk W, Osswald TA (2022) Manufacturing of a PET Filament from Recycled Material for Material Extrusion (MEX), *Recycling*, vol. 7, no. 5, p. 69. 10.3390/recycling7050069
21. Seno Flores JD, de Assis Augusto T, Lopes Vieira Cunha DA, Gonçalves Beatrice CA, Henrique Backes E, Costa LC (2024) Sustainable polymer reclamation: recycling poly(ethylene terephthalate) glycol (PETG) for 3D printing applications. J Mater Science: Mater Eng 19(1). 10.1186/s40712-024-00163-x
22. Ror CK, Negi S, Mishra V (2023) Development and characterization of sustainable 3D printing filaments using post-consumer recycled PET: processing and characterization. J Polym Res 30(9):350. 10.1007/s10965-023-03742-2
23. Petousis M et al (Sep 28 2023) A Coherent Assessment of the Compressive Strain Rate Response of PC, PETG, PMMA, and TPU Thermoplastics in MEX Additive Manufacturing. Polym (Basel) 15(19):3926. 10.3390/polym15193926
24. Ergene B, Bolat Ç (2022) An Experimental Investigation on the Effect of Test Speed on the Tensile Properties of the Petg Produced by Additive Manufacturing, *International Journal of 3D Printing Technologies and Digital Industry*, vol. 6, no. 2, pp. 250–260. 10.46519/ij3dptdi.1069544
25. Mehtedi ME, Buonadonna P, El Mohtadi R, Loi G, Aymerich F, Carta M (2024) Optimizing Milling Parameters for Enhanced Machinability of 3D-Printed Materials: An Analysis of PLA, PETG, and Carbon-Fiber-Reinforced PETG. J Manuf Mater Process 8(4). 10.3390/jmmp8040131
26. Ghasemkhani A, Pircheraghi G, Mehrabadi NR, Eshraghi A (2024) Effects of heat treatment on the mechanical properties of 3D-printed polylactic acid: Study of competition between crystallization and interlayer bonding. Mater Today Commun 39:109266. 10.1016/j.mtcomm.2024.109266
27. Méndez JA et al (2007) Evaluation of the reinforcing effect of ground wood pulp in the preparation of polypropylene-based composites coupled with maleic anhydride grafted polypropylene. J Appl Polym Sci 105(6):3588–3596. 10.1002/app.26426
28. Munoz-Shuguli C, Moran D, Velasquez E, Lopez-Vilarino JM, Lopez-de-Dicastillo C (Sep 20 2025) Effect of Degradation During Multiple Primary Mechanical Recycling Processes on the Physical Properties and Biodegradation of Commercial PLA-Based Water Bottles. Polym (Basel) 17(18):2542. 10.3390/polym17182542
29. Nguyen PQK et al (2024) Influences of printing parameters on mechanical properties of recycled PET and PETG using fused granular fabrication technique. Polym Test 132:108390. 10.1016/j.polymertesting.2024.108390
30. Mishra V, Ror CK, Negi S, Veeman D (2025) Recycling PET Waste into Functional 3D Printing Material: Effect of Printing Temperature on Physio-mechanical Properties of PET Parts. J Mater Eng Perform 34(22):26778–26790. 10.1007/s11665-025-11184-8

31. Pires P, Aguiar MLd, Vieira AC (2025) Mechanical Performance of rPET Filament Obtained by Thermal Drawing for FFF Additive Manufacturing. J Manuf Mater Process 9(1):26. 10.3390/jmmp9010026

Figures

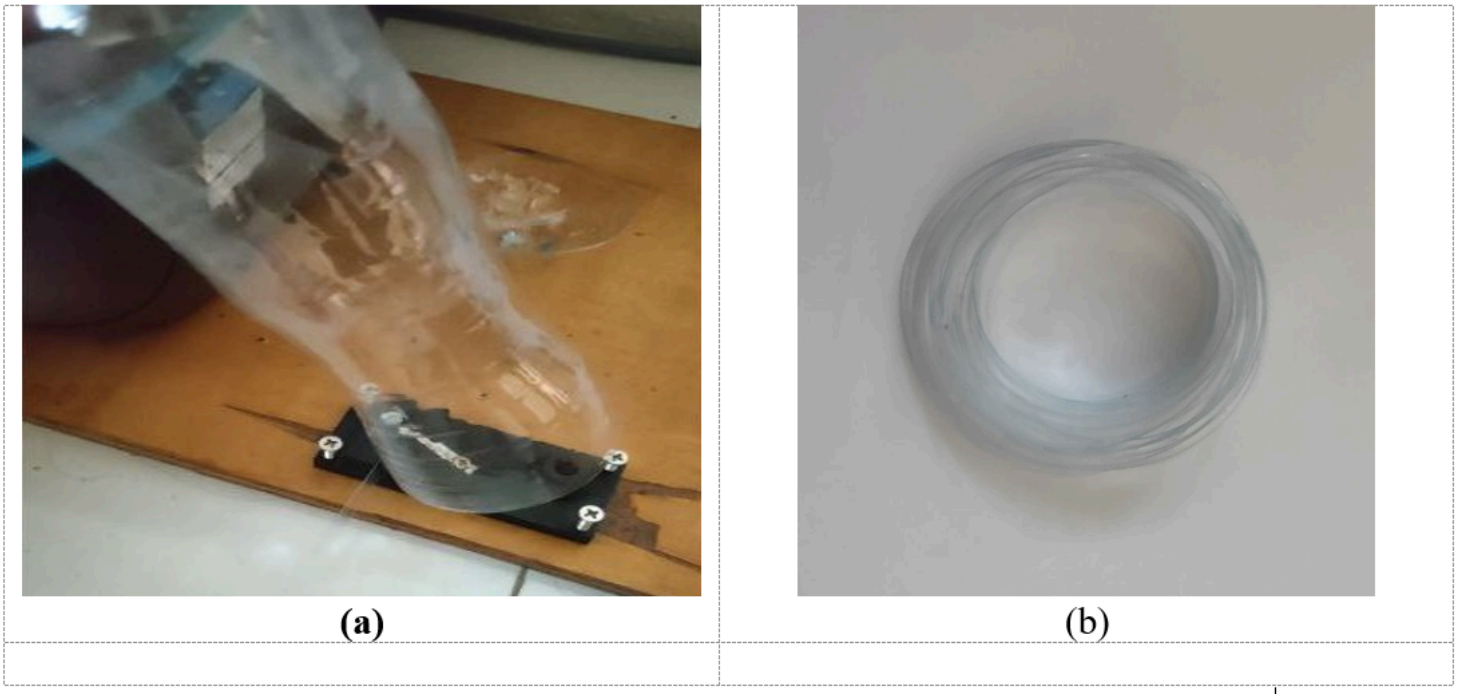


Figure 1

Preparation of recycled PET feedstock. (a) Coiled PET filament produced from bottle strips. (b) Bottle-stripping process showing continuous removal of PET ribbon from a post-consumer bottle.

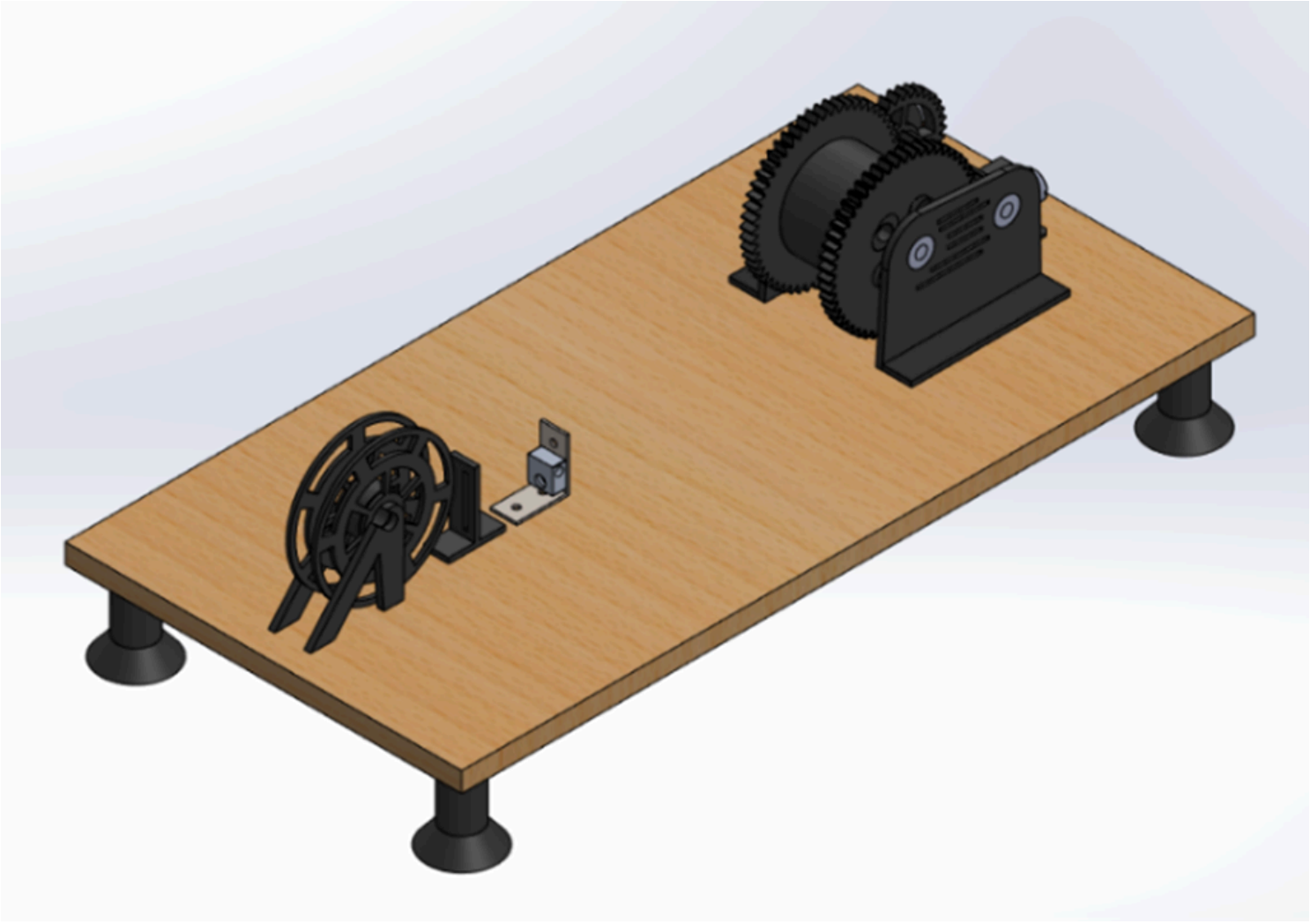


Figure 2

CAD model of the PET filament extruder created in SolidWorks, illustrating the gear motor assembly and alignment of the heating zone.

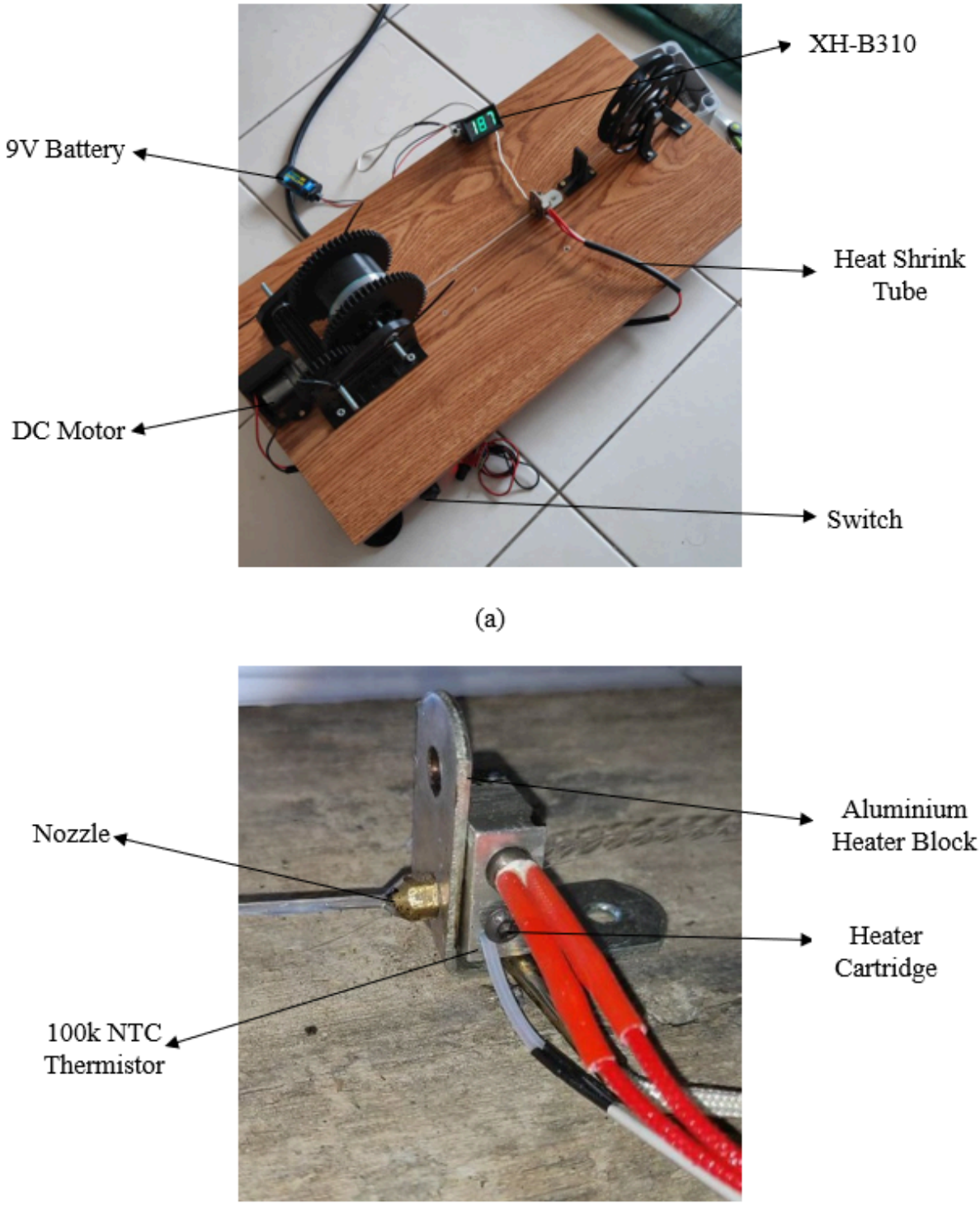


Figure 3

Fabricated low-cost PET extruder prototype: (a) Overall extruder assembly; (b) Close-up of the hot-end section showing the heater block, nozzle, and temperature-control components.

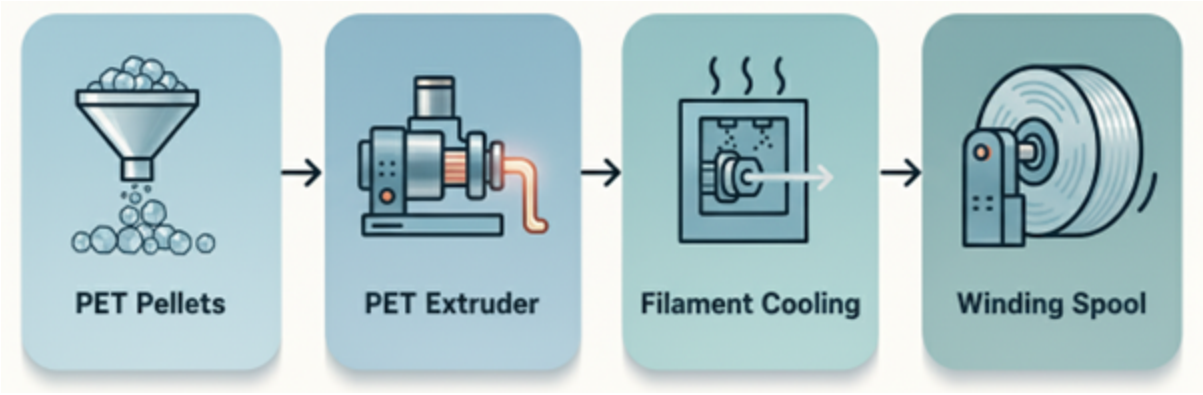


Figure 4

Schematic representation of the key stages involved in converting PET bottle strips into filament through the extrusion process, including material feeding, extrusion, cooling, and winding.

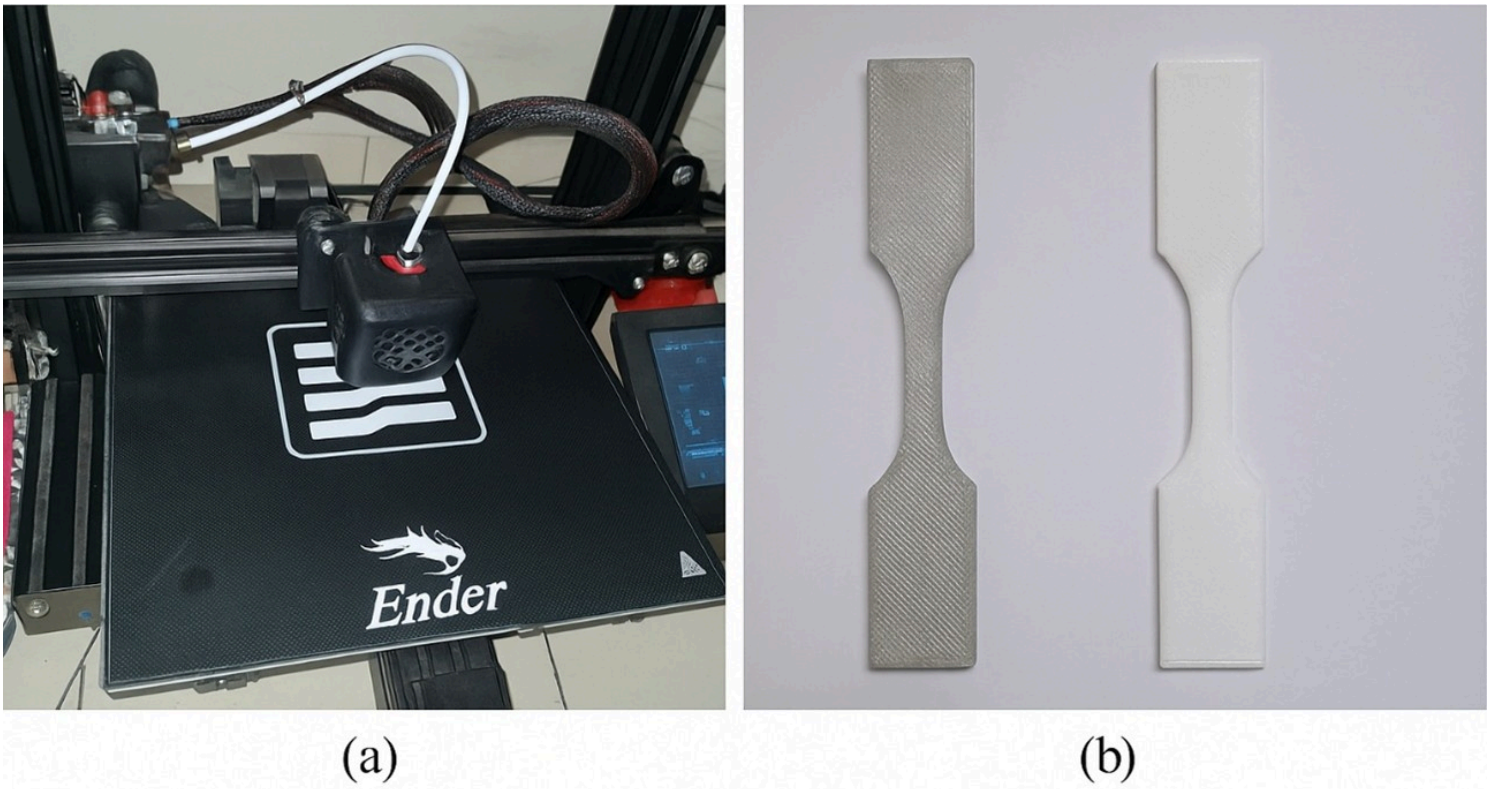


Figure 5

3D-printed ASTM D638 Type V tensile specimens: (a) Commercial PETG specimen fabricated for benchmarking **(b) Recycled PET and Commercial PETG filament specimen.**



Figure 6

Tensile testing setup using the Shimadzu Servopulser universal testing machine (5 kN load cell).

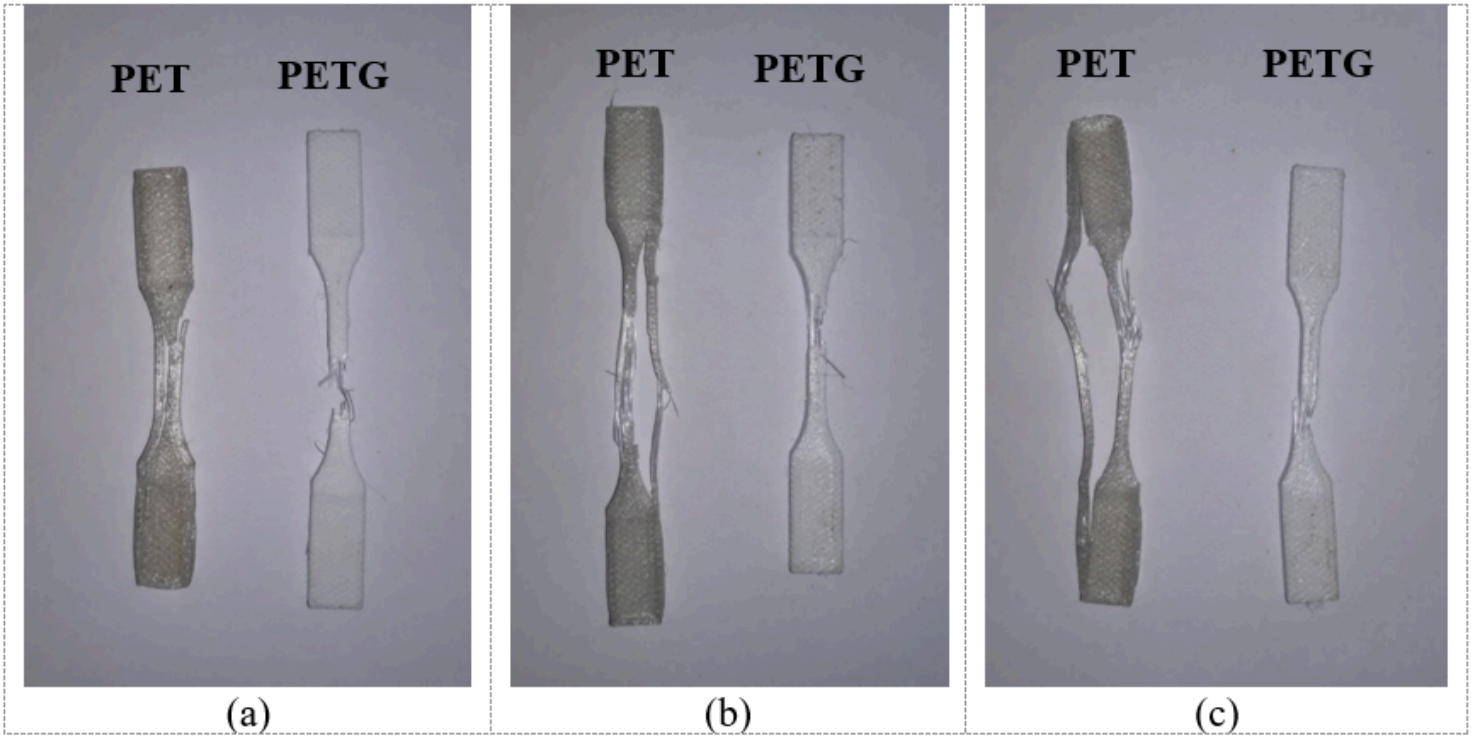


Figure 7

Tensile fracture surfaces of PET and PETG at 1–5 mm/min, showing brittle failure in PET and ductile necking in PETG.

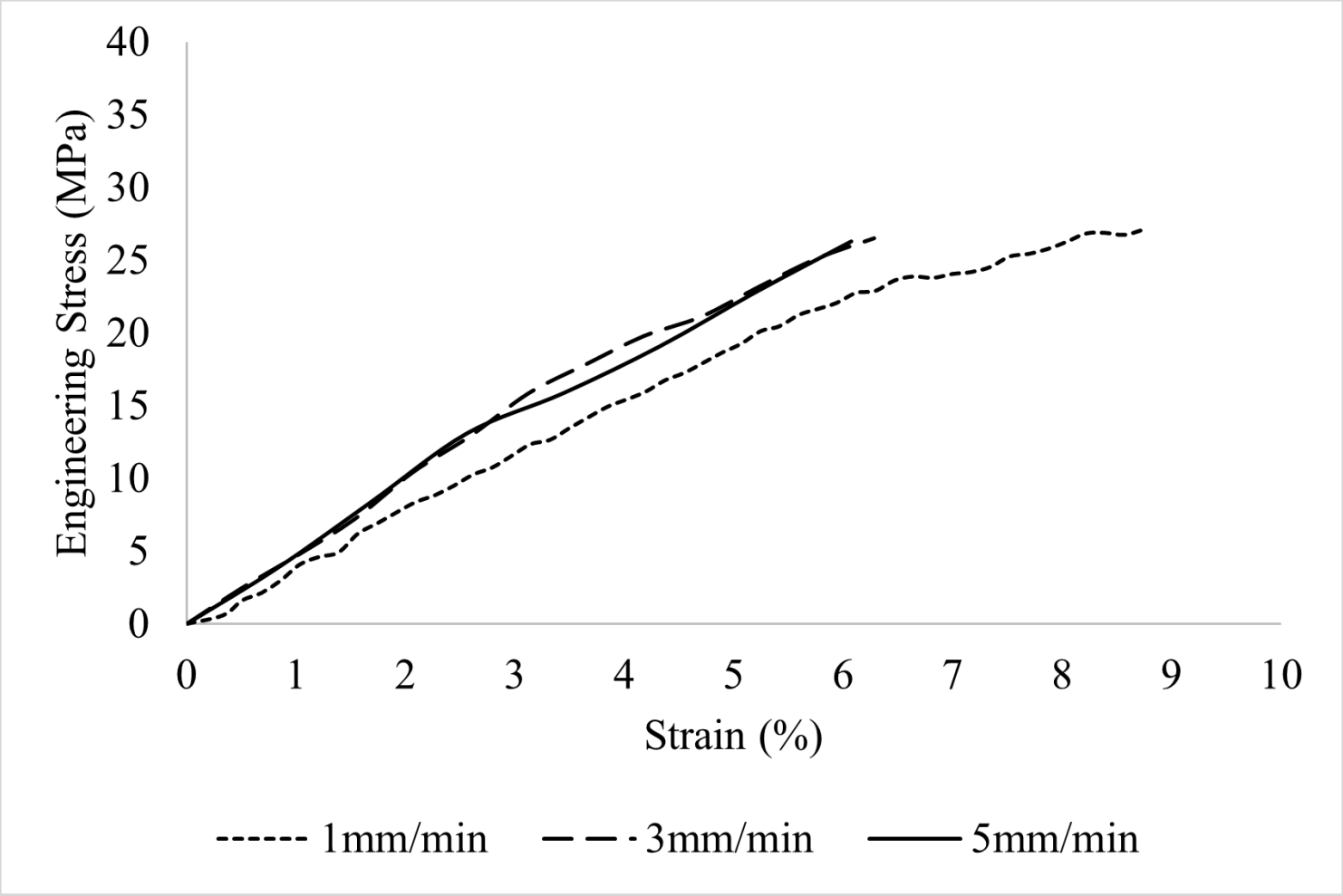


Figure 8

Engineering stress–strain curves for recycled PET (rPET) tested at crosshead speeds

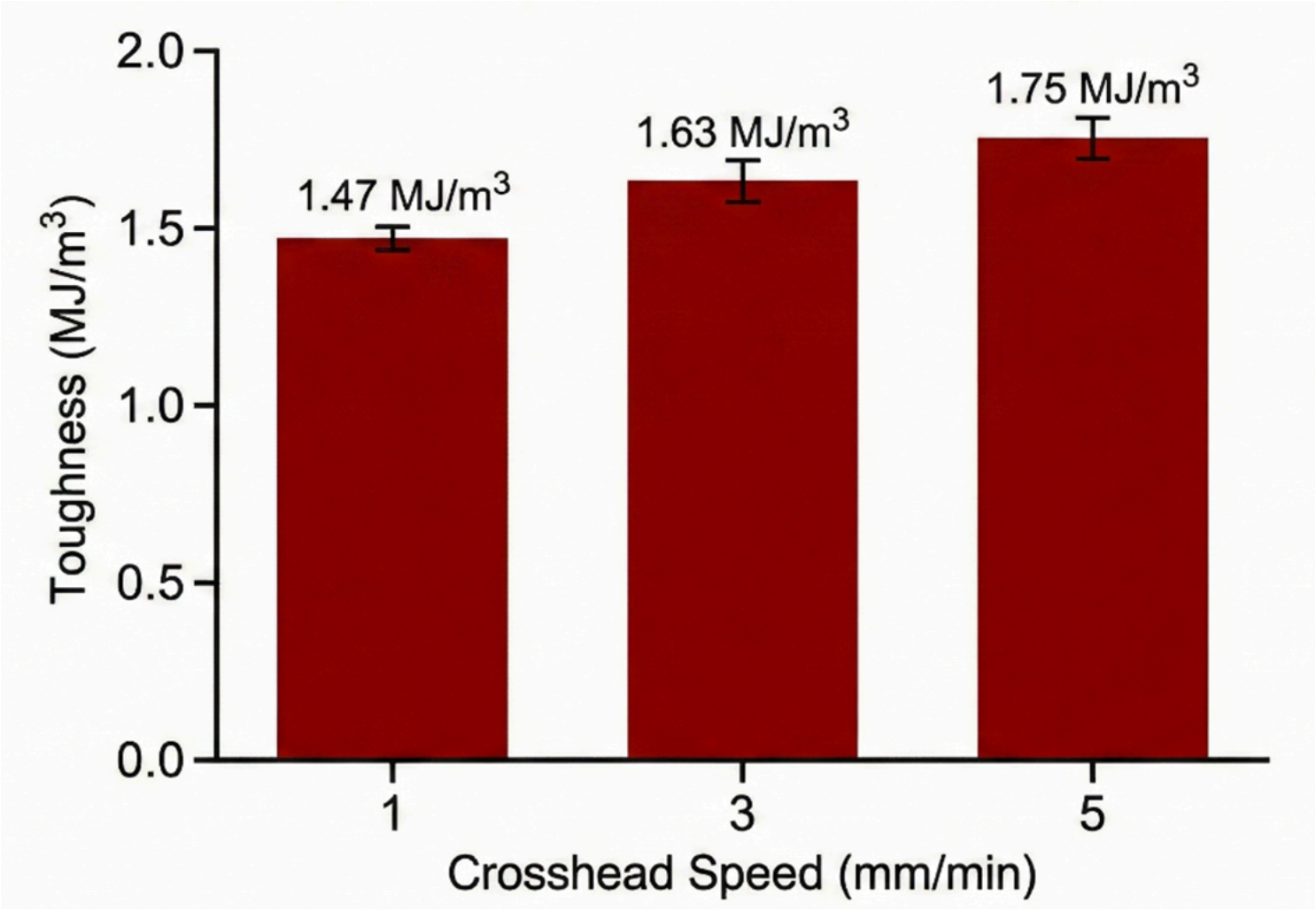


Figure 9

Strain-rate dependence of toughness (strain energy density) for commercial PETG, calculated from integrated engineering stress–strain curves at crosshead speeds of 1, 3, and 5 mm/min. The results demonstrate the ability of PETG to maintain and progressively enhance energy absorption with increasing loading rate.

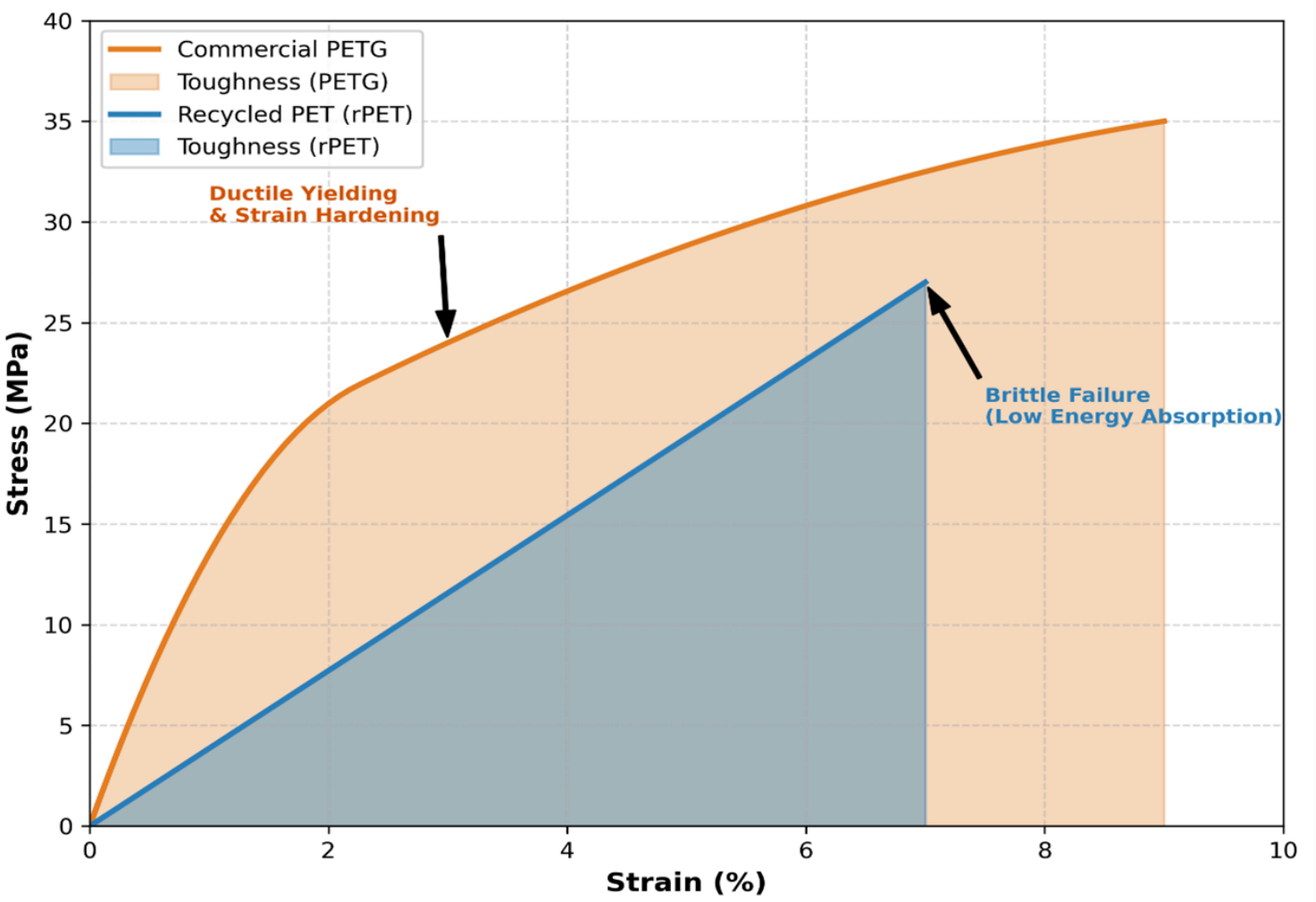


Figure 10

Comparative stress–strain behaviour of recycled PET versus commercial PETG at a constant crosshead speed of 1 mm/min. The shaded areas represent the modulus of toughness (total energy absorption), visually highlighting the trade-off between the high stiffness/brittle failure of rPET (blue) and the superior ductility/energy dissipation of PETG (orange).

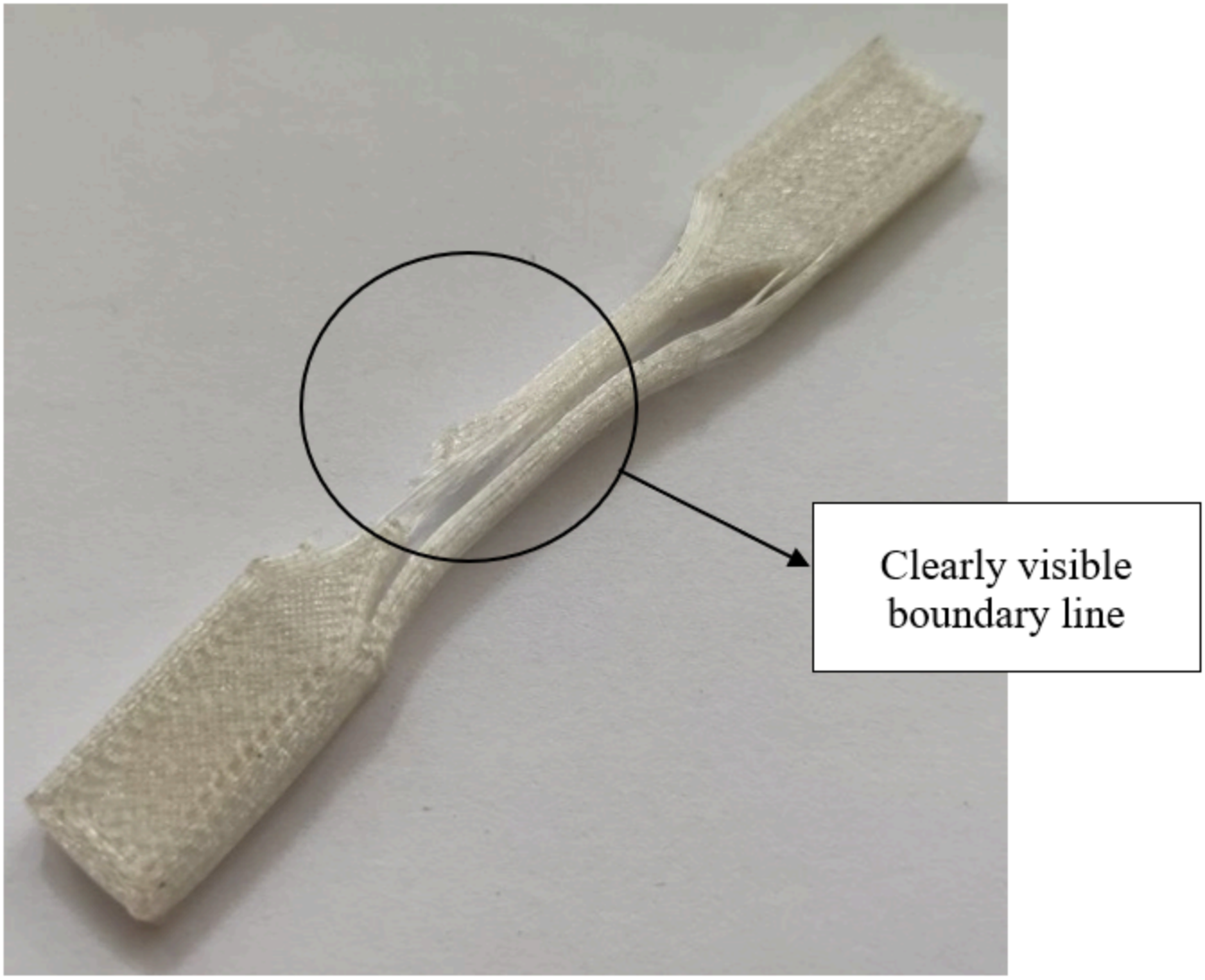


Figure 11

Macroscopic fracture morphology of the recycled PET (rPET) specimen tested at a crosshead speed of 5 mm/min, highlighting the sharp, granular surface and absence of necking characteristic of brittle failure.

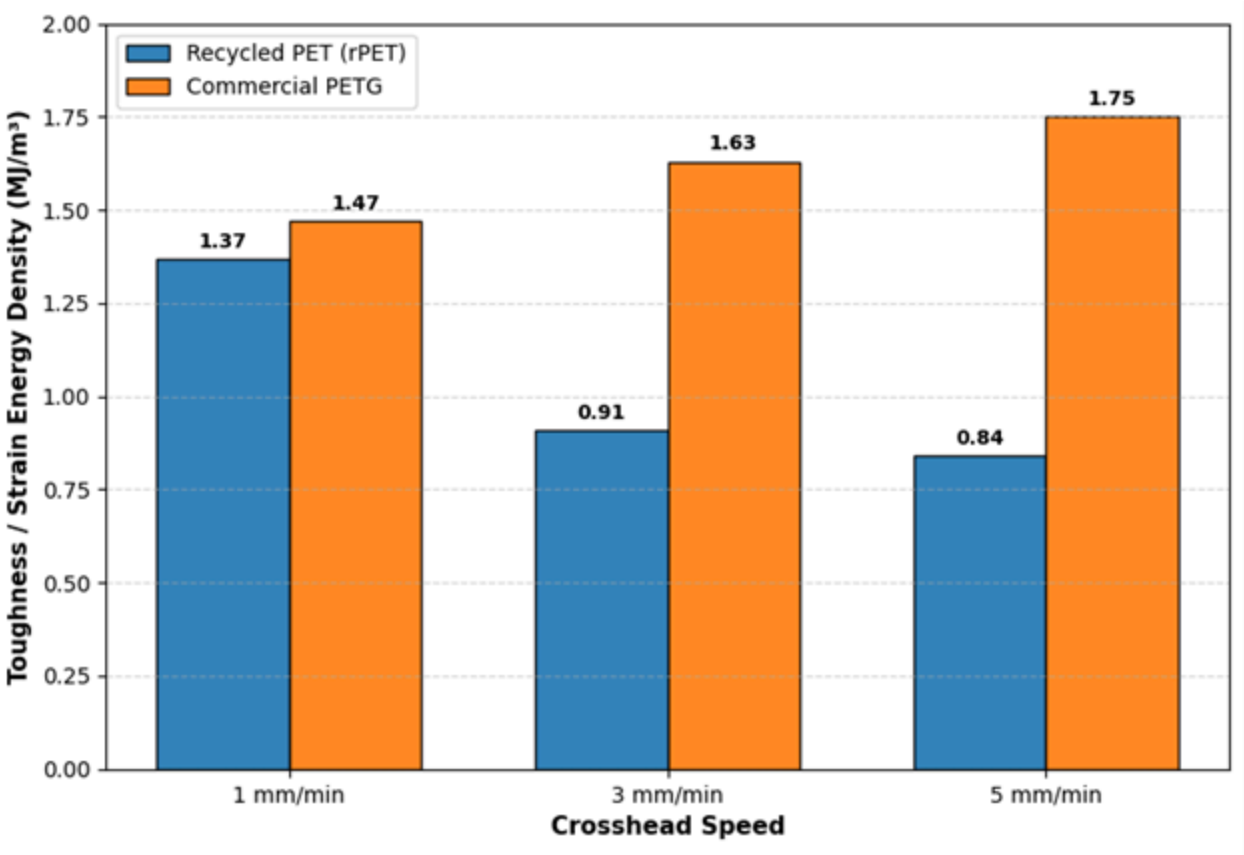


Figure 12

Comparative Toughness (strain energy density) of recycled PET and commercial PETG at varying crosshead speeds, calculated from integrated stress–strain data.

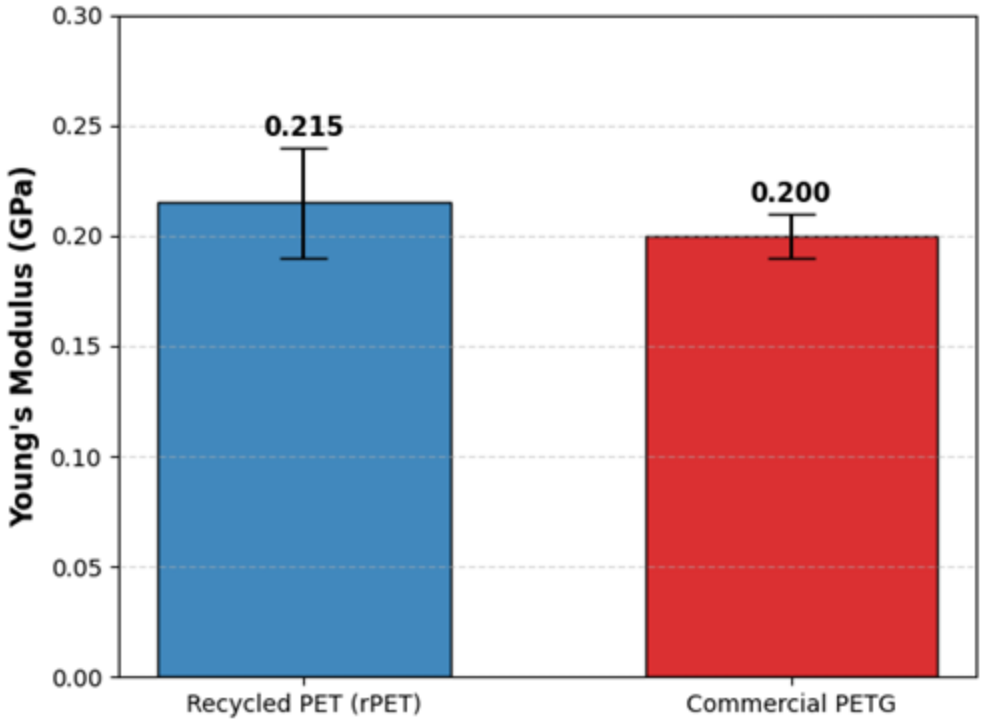


Figure 13

Comparative Young's modulus of recycled PET (rPET) and commercial PETG, showing the higher elastic stiffness of rPET associated with its semi-crystalline structure.

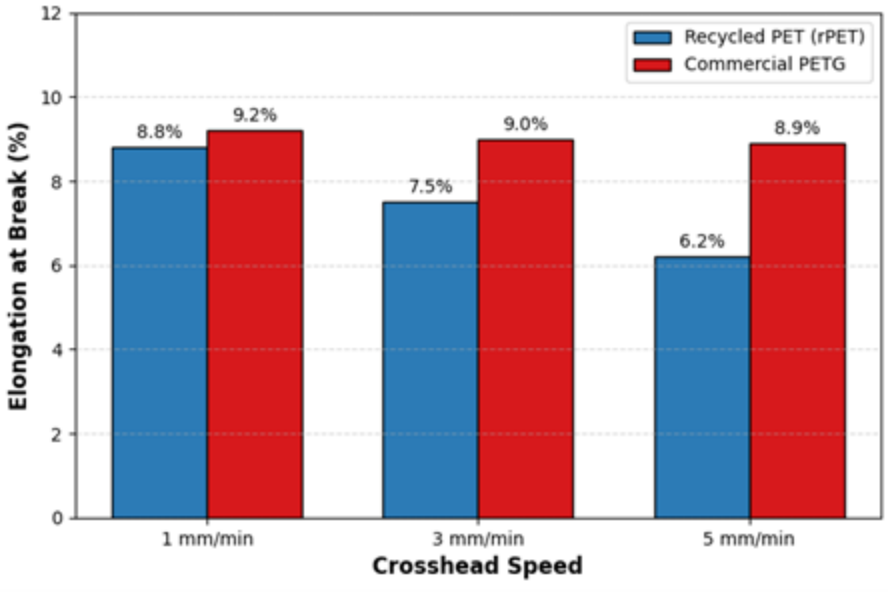


Figure 14

Elongation at break of recycled PET and commercial PETG as a function of crosshead speed, illustrating the contrasting strain-rate sensitivity of rPET and the retained ductility of PETG across all tested loading rates.

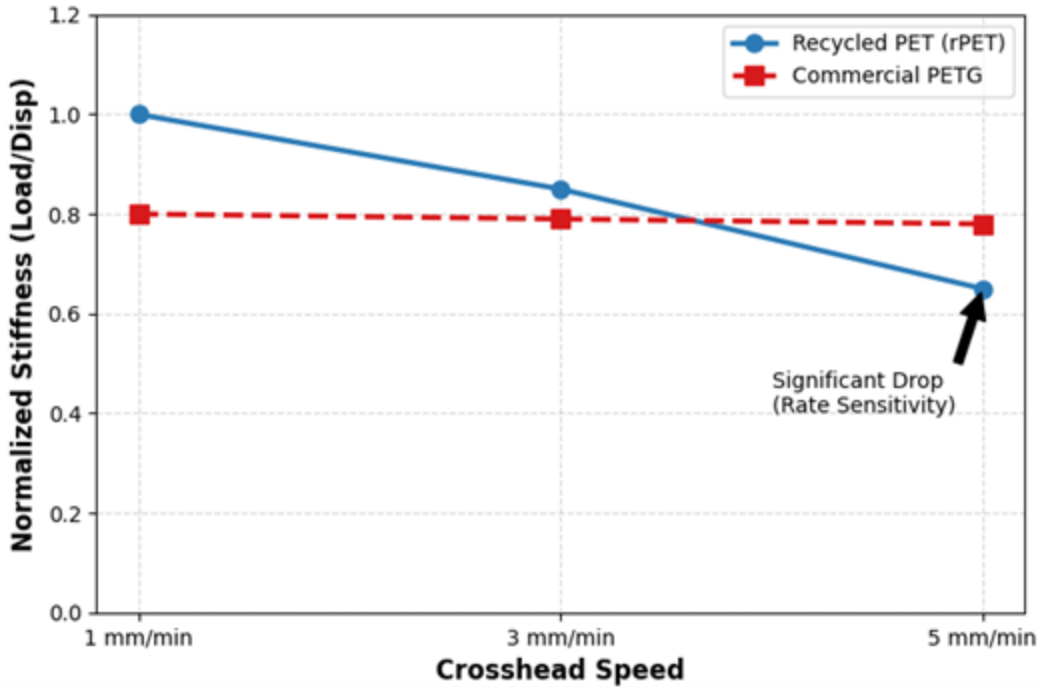


Figure 15

Normalized Stiffness Stability (Load/Displacement) as a function of loading rate, illustrating the strain-rate sensitivity of rPET compared to PETG.